

Electron spin resonance (ESR) spectra of amphiphilic spin probes in the triblock copolymer EO₁₃PO₃₀EO₁₃ (Pluronic L64): hydration, dynamics and order in the polymer aggregates

L. Zhou¹, S. Schlick*

Department of Chemistry, University of Detroit Mercy, 4001 W. McNichols Road, PO Box 19900, Detroit, MI 48219, USA

Received 1 April 1999; received in revised form 12 August 1999; accepted 17 August 1999

Abstract

Aqueous solutions of the triblock copolymer poly(ethylene oxide)-*b*-poly(propylene oxide)-*b*-poly(ethylene oxide) EO₁₃PO₃₀EO₁₃ (Pluronic L64) were investigated over a wide concentration range (20–100%, (w/w) polymer) in the micellar, liquid crystalline and reverse micellar phases, using electron spin resonance (ESR) spectroscopy of spin probes. A series of amphiphilic nitroxide spin probes based on *n*-doxyl-stearic acid (*n*DSA) with *n*, the carbon atom to which the doxyl group is attached, equal to 5 and 10 were used to measure the local polarity, dynamics and degree of order in the self-assembled system. The ¹⁴N isotropic hyperfine splitting, *a*_N, was the polarity sensitive parameter. The probe location and the corresponding *effective* local hydration, *Z*_{eff}, were deduced by comparing ESR spectra of the probes in L64 solutions with spectra of the probes in aqueous solutions of poly(ethylene oxide) (PEO), poly(propylene oxide) (PPO) and a mixture of PEO and PPO containing the monomer molar ratio 26:30, as in L64. The results indicate that the probes reside in and provide evidence for the presence of hydrophobic and non-hydrated regions consisting of PO blocks and that the order in the aggregates decreases from the PO/EO interface toward the PO domains. Additional support for these conclusions was obtained from ESR spectra of the probes in the lamellar phase as a function of added cholesterol and by simulations of the ESR spectra of the probes in the lamellar phase of L64. This study of the hydrophobic part of the aggregates, together with our previous study based on ESR spectra of cationic probes that reside in the polar and hydrated EO regions, lead to a detailed description of the nature of L64 aggregates in aqueous solutions. © 2000 Elsevier Science Ltd. All rights reserved.

Keywords: Pluronic triblock copolymers; Spin probes; Self-assembly

1. Introduction

The triblock copolymers poly(ethylene oxide)-*b*-poly(propylene oxide)-*b*-poly(ethylene oxide) (EO_{*m*}PO_{*n*}EO_{*m*}), available commercially as Synperonics, Pluronics or Poloxamers, have attracted great interest because of their diverse and complex structures in aqueous solutions and their applications in drug release systems, detergents, cosmetics, treatment of burns and water purification [1–4]. The copolymers can also be prepared with a central EO block flanked by two PO blocks (“reverse Pluronics”), or in a dendrimer architecture with PEO–PPO or PPO–PEO diblocks linked to an ethylenediamine core [5].

Micelles, reverse micelles and liquid crystalline mesophases have been detected in many Pluronics,

depending on temperature and polymer composition and concentration [1–4,6–17].^{2,3} In the isotropic micellar phase, the critical micelle concentration (CMC) has an inverse temperature dependence; at a given concentration the appearance of the micelles is gradual over a relatively broad temperature range, due to the polydispersity of the PO and EO blocks and to the combined effects of polymer size and increased hydrophobicity of both blocks with temperature [6–17]. The CMC and the critical micellization temperature (CMT) decrease with increase of the PO content and of the molecular weight [18]. In the simplest picture the micellar core is expected to consist of PO blocks and the corona of EO blocks; some experiments and theoretical models suggest, however, that the segregation

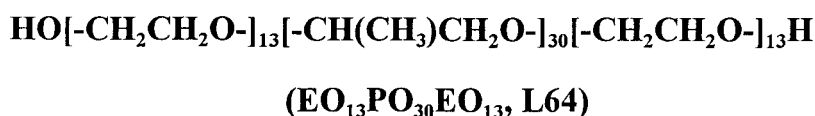
* Corresponding author. Tel.: +1-313-993-1012; fax: +1-313-993-1144.
E-mail address: schlicks@udmercy.edu (S. Schlick).

¹ Present address: Essex Specialty Products, 1250 Harmon Road, Auburn Hills, MI 48236, USA.

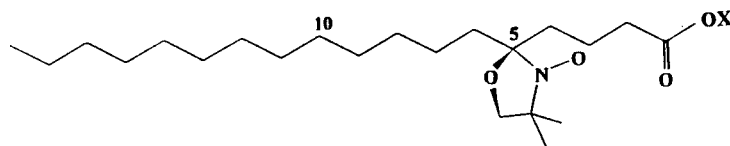
² Ref. [8] presents the phase diagram of a reverse Pluronic (EO block in the middle) in water–oil mixtures.

³ In Ref. [11] the phase diagram for L64 is more accurate and detailed compared to that published previously in Ref. [9].

Chart 1: Pluronic L64 and Spin Probes



Spin Probes



n-Doxyl Stearic Acid Spin Probes:

X=H: *n*DSA (*n*=5,10)

X=CH₃: *n*DSE (*n*=10)

Scheme 1.

between the core and the corona is not complete and that the core may also contain EO units [15–17].

The self-assembly of the Pluronics is similar to that of the non-ionic surfactants of the oligo(ethylene oxide) $C_m\text{EO}_n$ type (C_m is an aliphatic chain with m carbon atoms); there are important differences, however, between the two systems: While the phase separation into the hydrophilic corona and the hydrophobic core in $C_m\text{EO}_n$ is clearly defined [19,20], important questions remain on the hydration of the two components (EO and PO) in the Pluronics and the degree of order in the self-assembled phases [21].

We have initiated a study of the Pluronic copolymers

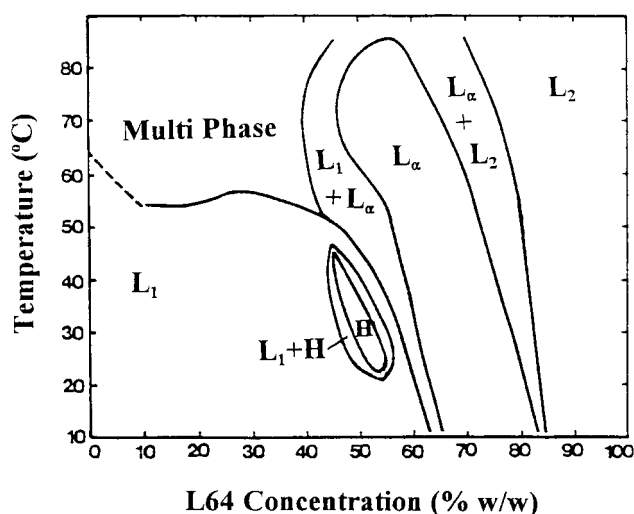


Fig. 1. Phase diagram for aqueous $\text{EO}_{13}\text{PO}_{30}\text{EO}_{13}$ (Pluronic L64). L_1 is the micellar phase, H is the hexagonal phase, L_α is the lamellar phase and L_2 is the reverse micellar phase. Dotted lines indicate the uncertainty in the phase boundaries (redrawn from Ref. [11]).

based on the ESR spectra of spin probes that are known to intercalate in and report on various regions of the self-assembled system. The main objectives of these studies are to obtain *local* information on the hydration of the hydrophobic and hydrophilic domains, on the degree of order in the aggregates and on the transport of various guests in the system [22–24]. Most of our studies have focused on $\text{EO}_{13}\text{PO}_{30}\text{EO}_{13}$ (commercial name L64, Scheme 1), whose phase diagram in aqueous solutions has been deduced by ^2H NMR, polarizing microscopy and ocular inspection [9,11]. In the vicinity of 300 K, the main phases detected with increasing polymer content are L_1 (micellar), H (hexagonal), L_α (lamellar) and L_2 (reverse micellar), as shown in Fig. 1. The size of the aggregates has been determined by dynamic light scattering [12–14] and small-angle X-ray scattering (SAXS) [11]. The radius of the micelles in the L_1 phase is in the range 60–80 Å; the radius of the cylinder in the hexagonal phase is ≈ 30 Å; in the lamellar phase the thickness of the apolar domain is in the range 30–40 Å and the periodicity is ≈ 80 Å.

The present paper describes results based on ESR spectra of amphiphilic doxyl stearic acid spin probes (*n*DSA, Scheme 1) in L64 and on spectral simulations of the ESR lineshapes in the lamellar phase. The following experimental parameters were varied in this study: the temperature, the L64 content in the solutions, the polarity of the probe head group (10DSA vs. the corresponding methyl ester, 10DSE), the position of the nitroxide with respect to the head group (5DSA vs. 10DSA) and the polarity of the solvent (water vs. 0.1 M NaOH aqueous solution). In addition, the effect of a wedge-shaped additive such as cholesterol on the ESR spectra of 5DSA was measured in the lamellar phase. The order parameter S in the lamellar phase was deduced from simulations of the ESR spectra of 5DSA, 10DSA and

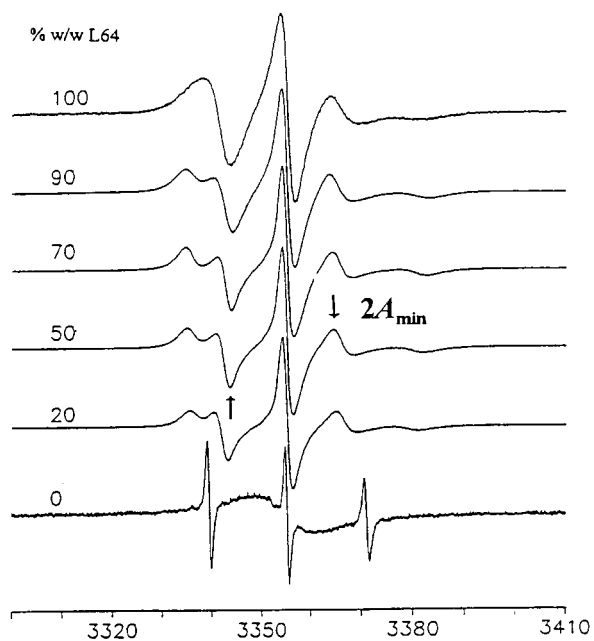
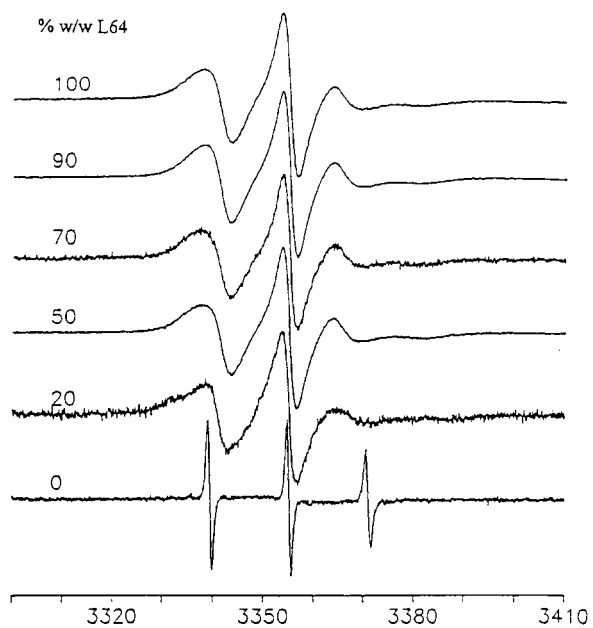
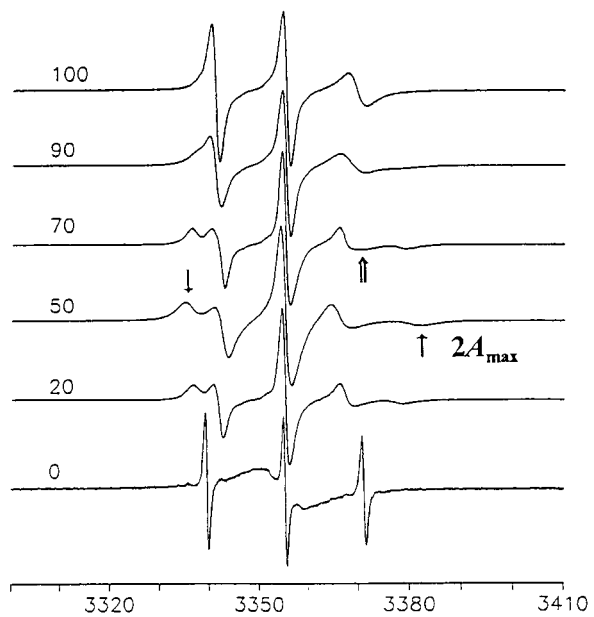
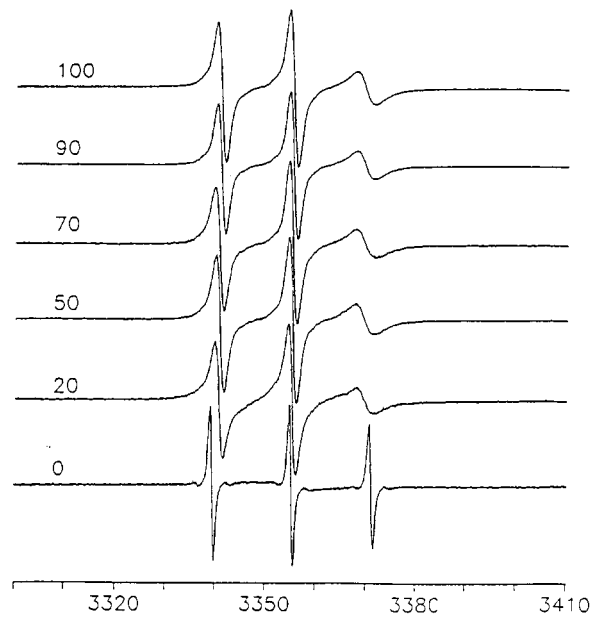
(A) 5DSA/L64/NaOH, 300 K**(B) 5DSA/L64/water, 300 K****(C) 5DSA/L64/NaOH, 325 K****(D) 5DSA/L64/water, 325 K****Magnetic Field (G)**

Fig. 2. X-band ESR spectra of 5DSA as a function of L64 content: in 0.1 M NaOH solutions at 300 K (A) and at 325 K (C) and in water solutions at 300 K (B) and at 325 K (D).

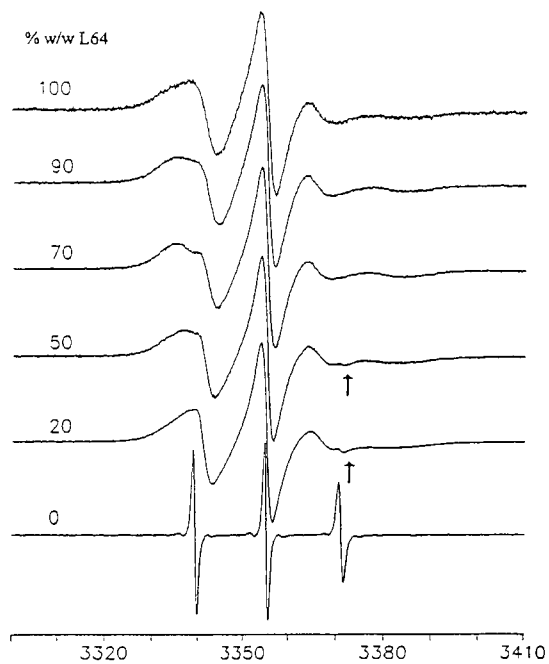
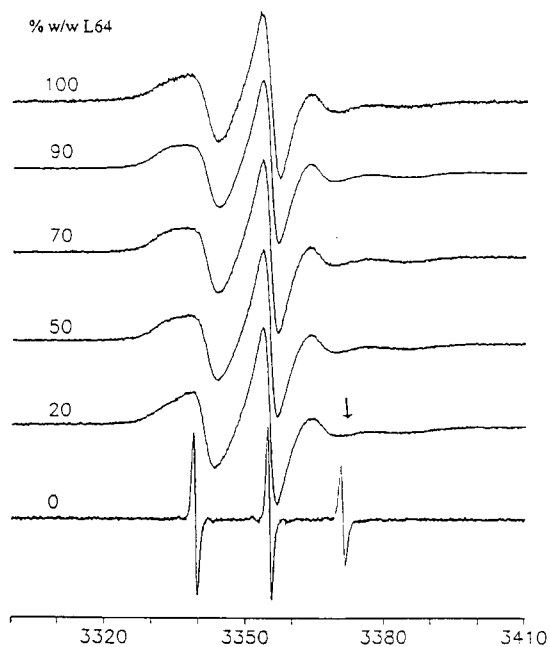
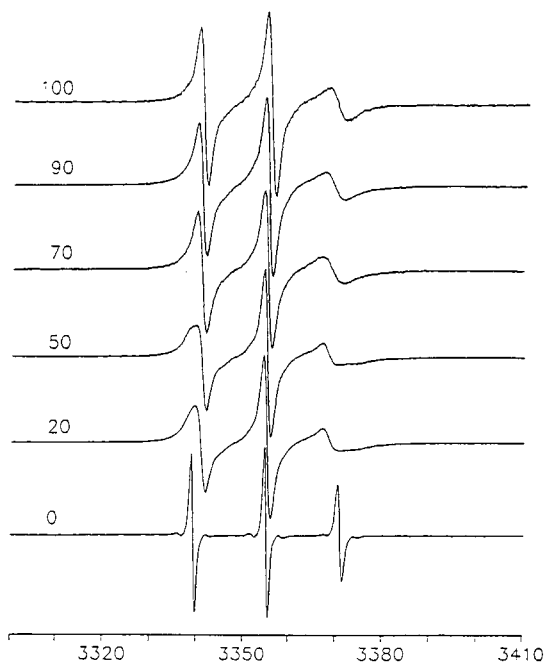
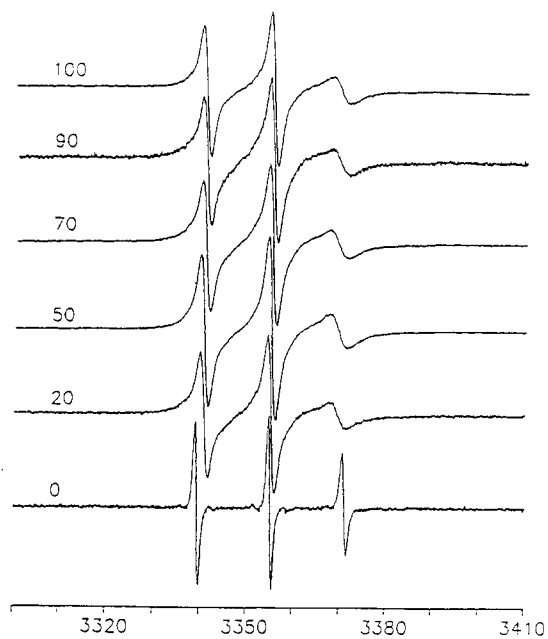
(A) 10DSA/L64/NaOH, 300 K**(B) 10DSA/L64/water, 300 K****(C) 10DSA/L64/NaOH, 325 K****(D) 10DSA/L64/water, 325 K****Magnetic Field (G)**

Fig. 3. X-band ESR spectra of 10DSA as a function of L64 content: in 0.1 M NaOH solutions at 300 K (A) and at 325 K (C) and in water solutions at 300 K (B) and at 325 K (D).

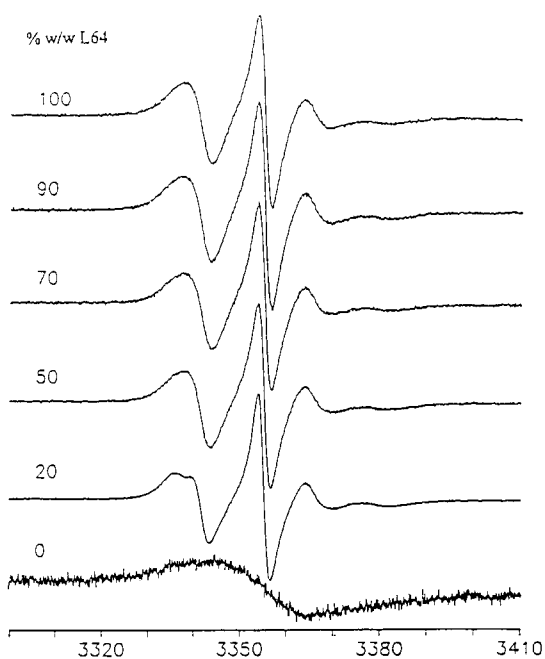
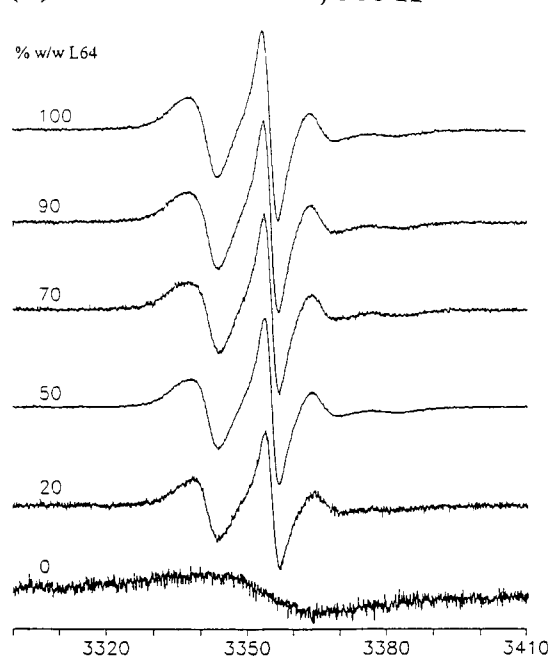
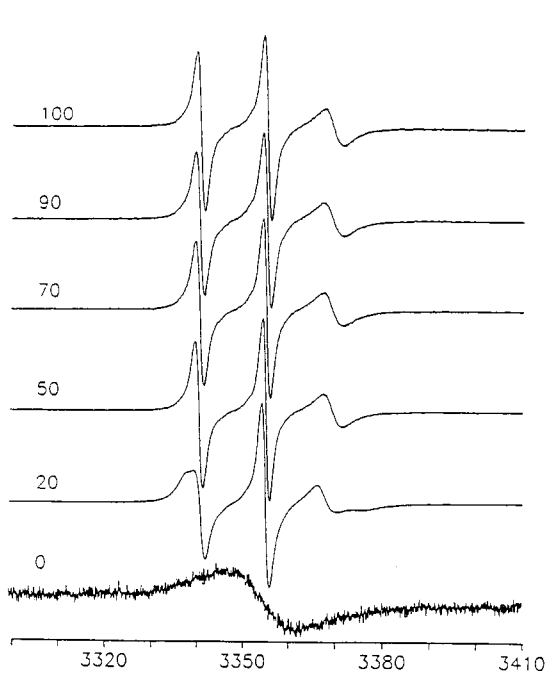
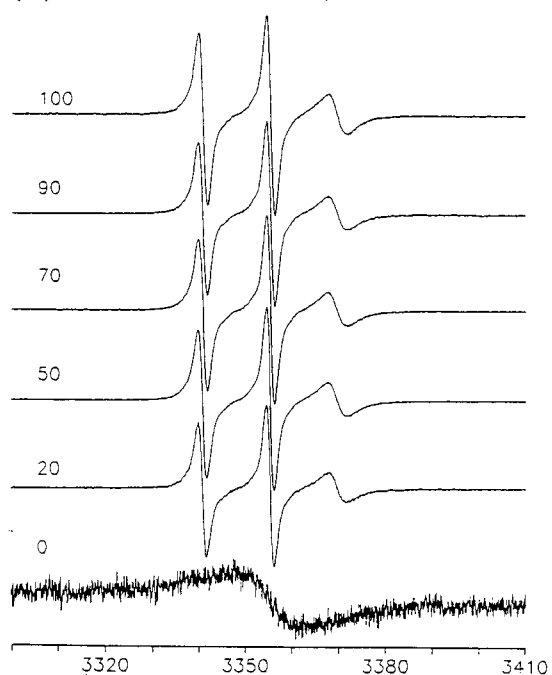
(A) 10DSE/L64/NaOH, 300 K**(B) 10DSE/L64/water, 300 K****(C) 10DSE/L64/NaOH, 325 K****(D) 10DSE/L64/water, 325 K****Magnetic Field (G)**

Fig. 4. X-band ESR spectra of 10DSE as a function of L64 content: in 0.1 M NaOH solutions at 300 K (A) at 325 K (C) in water solutions at 300 K (B) at 325 K (D).

10DSE at 300 K. Preliminary results have been reported [25].

2. Experimental

2.1. Materials

The copolymer L64, with nominal molecular weight 2900 and EO content of 40% (w/w) was a gift from BASF Corporation and was used as received. The spin probes 5DSA and 10DSA (from Aldrich) and 10DSE (from Molecular Probes, Eugene, OR) were used as received. Poly(ethylene oxide) (Carbowax300 from Union Carbide, MW 300) and poly(propylene oxide) (PPG425 from ARCO Chemical Company, MW 425) were also gifts and were used as received.

2.2. Sample preparation

Solutions of L64 in water or in 0.1 M NaOH were prepared by weighing appropriate amounts in 8 mm i.d. tubes, which were sealed immediately and centrifuged repeatedly in both directions during 1 week to facilitate mixing [8–10]. The liquid crystalline phases were solid-like gels and their appearance was checked by examination between crossed polarizers.

The spin probes were dissolved in ethanol to a concentration of ≈ 5 mM and divided into several vials [26]. After evaporation of the solvent overnight in air or in a stream of nitrogen, the spin probe film was dissolved in neat or aqueous L64. The solution was shaken by hand for several minutes, kept in the refrigerator overnight, transferred to capillaries made from disposable pipettes and flame-sealed for the ESR experiments. The spin probe concentration in the polymer solutions was ≈ 0.5 mM, low enough to prevent linewidth broadening by spin–spin interactions: further lowering of the spin probe concentration had no effect on the ESR linewidths. Probes in two types of L64 solutions were prepared, in water and in aqueous 0.1 M NaOH; the carboxylic groups of 5DSA and 10DSA spin probes are in the undissociated acid form COOH in the former solutions and in the ionized form COO[−] in the latter. The pH of the L64 solutions was 11.8, 9.8, 7.5, 6.9 and 6.4 for polymer contents of 20, 50, 70, 90 and 100% w/w, respectively. No effect on the phase diagram was detected in the basic L64 solutions compared to the neat water solutions [23]. As will be seen later, the ionization of the carboxylic group has important effects on the ESR spectra of the probes.

For determination of the local degree of hydration [22–24], a_N values of 5DSA were measured in aqueous solutions of the homopolymers PEO and PPO as a function of $Z = [\text{water}]/[\text{monomer}]$, the number of water molecules per EO or PO unit. In order to mimic as closely as possible the local environment in L64, a_N values of 5DSA were also measured as a function of Z in a mixture of the

homopolymers containing a EO:PO molar ratio 26:30, as in L64; in these mixtures Z refers to the total number of monomer units, EO–PO.

2.3. ESR measurements

ESR spectra were measured with a Bruker ECS106 spectrometer equipped with the ESP 3240 data system for acquisition and manipulation and with the ER4121 VT variable temperature unit. The microwave frequency was measured with the Hewlett-Packard 5342A microwave counter. Spectra were measured with 100 kHz magnetic field modulation, modulation amplitude 0.4 G, microwave power 2 mW and 10 scans. The ¹⁴N isotropic hyperfine splitting, a_N , was measured directly from the spectra for motionally narrowed lineshapes, or from $a_N = (A_{\text{max}} + 2A_{\text{min}})/3$, where A_{max} and A_{min} are determined from the experimental spectra, as shown by arrows in Fig. 2.

2.4. Spectral simulations

The principal values of the g - and ¹⁴N-hyperfine tensors for the spin probes cannot be determined from the rigid-limit spectra measured at 77 K, because of the very broad lines. For this reason, we adopted the components of the g tensor determined for the doxyl probes in lyophilized bovine serum albumin (BSA): [27,28] $g_{xx} = 2.0088$, $g_{yy} = 2.0066$, $g_{zz} = 2.0027$ for all probes. The components of the ¹⁴N hyperfine tensor were selected using the *scaling procedure* [28]. The values determined in lyophilized BSA ($A_{xx}(\text{BSA}) = 6.3$ G, $A_{yy}(\text{BSA}) = 5.8$ G, $A_{zz}(\text{BSA}) = 33.5$ G) were scaled to fit the experimental isotropic hyperfine constant. The scaling procedure was performed for $a_N = 14.8$ G (compared to 15.2 G in BSA). The tensor components $A_{xx} = 6.1$ G, $A_{yy} = 5.7$ G, $A_{zz} = 32.6$ G obtained from this procedure were used for simulating the ESR spectra.

We simulated ESR spectra of the probes in L64 solutions for a polymer concentration corresponding to the lamellar phase (L_{α} , 70% (w/w) L64), because the dynamical model is dictated by the organized phase: the obvious choice is the microscopic order–macroscopic disorder model (MOMD), which implies that the spin probe reorients in the presence of an ordering potential λ due to the surrounding molecules, characterized by a director d [29]. In the absence of macroscopic order, d is expected to be distributed at random. For this reason the simulated spectrum is obtained by a superposition of spectral components weighted by $\sin \theta$ for angles θ between the direction of the external magnetic field H and the director d . Typically 30 θ values in the interval 0–90° were calculated and superimposed. Spectra were calculated on a 586/100 MHz PC, using the EPRL set of programs [30].⁴ Each spectrum required ≈ 7 min of computer time.

⁴ The EPRL version 1.6 has been kindly provided by Dr D.E. Budil of Northeastern University, Boston, MA.

Table 1
¹⁴N hyperfine splittings, a_N (G), at 325 K of *n*DSA and 10DSE probes in L64/water^a

Phase	L64 (wt%)	5DSA	10DSA	10DSE	Z [H ₂ O]/[EO]
	0	15.8 (15.8)	15.8 (15.8)	^c	
L ₁	20	14.8 ^b (14.4)	14.3 (14.3)	14.3 (14.3) ^d	24.8
L ₁ + L _α	50	14.8 ^b (14.4)	14.1 ^b (14.4)	14.3 (14.3)	6.2
L _α	70	14.8 ^b (14.4)	14.0 ^b (14.2)	14.3 (14.3)	2.7
L ₂	90	14.7 ^b (14.4)	14.2 (14.4)	14.3 (14.3)	0.7
	100	14.4 (14.4)	14.2 (14.3)	14.3 (14.3)	0
		Z _{eff} < 1	Z _{eff} ≈ 0	Z _{eff} ≈ 0	

^a For each probe we give the a_N (G) values in the NaOH solutions and in parentheses, the values in water solutions.

^b Calculated from A_{\min} and A_{\max} values; the estimated error is ± 0.15 G. The other values of a_N were read directly from the spectra; the estimated error in these values is ± 0.1 G.

^c Insoluble in water or 0.1 M NaOH.

^d Same a_N in water or 0.1 M NaOH solutions and independent of L64 content.

3. Results and discussion

The ESR spectra of the spin probes in L64 solutions were measured at 300 and 325 K. The use of L64 dissolved in 0.1 M NaOH instead of water may lead to some changes in the phase diagram, but from our previous work [24] it seems that the aggregate interior is little, if at all, affected by the modification of the pH; we note that in the reverse micelles based on AOT, the ESR spectrum of 5DSA is the same for solutions with pH values in the range 6.3–9.0 [31]. We will use the notation probe/water and probe/NaOH for samples that do not contain L64; L64/water and L64/NaOH for the polymer solutions; and probe/L64/water and probe/L64/NaOH for the polymer solutions containing the probes.

3.1. Aggregate regions reported by the spin probes

X-band ESR spectra at 300 and 325 K for 5DSA, 10DSA and 10DSE in L64/water and L64/NaOH systems are presented in Figs. 2–4. The rich display of spectral features reflects the different phases at a given temperature, the specific site for each probe and the effect of temperature on the dynamics. These features will be discussed for each probe.

(a) 5DSA. At 300 K the ESR spectra of the probe in neat water consist of the isotropic triplet (Fig. 2B, lowest spectrum). The additional broad signal detected in aqueous NaOH (Fig. 2A, lowest spectrum) is assigned to probe aggregation: the probe has a lower CMC in the alkaline medium compared to neat water [32]. The spectra change dramatically upon addition of L64 and well-resolved lineshapes typical of the slow-motional regime are seen in the range of L64 concentrations 20–90% (w/w) in L64/NaOH; the lineshapes are not as well resolved in L64/water.

ESR spectra at 325 K reveal slow-motional lineshapes in the presence of NaOH (Fig. 2C) and motionally narrowed spectra in the absence of NaOH (Fig. 2D). The different dynamical regimes are clear evidence for different probe

sites in L64/NaOH and L64/water, due to the different pH values. A similar effect has been reported [33].⁵

The effect of temperature on probe dynamics is seen by comparing the corresponding spectra in the same solvent at 300 K and at 325 K, Fig. 2A with C and Fig. 2B with D. The extreme separation at 325 K in L64/NaOH is lower compared to that at 300 K; the only exception is the L64/NaOH solution containing 50% (w/w) copolymer, which has about the same extreme separation at both temperatures, a result that is difficult to interpret because of the presence of the hexagonal phase at 300 K and a mixture of L₁ + L_α at 325 K, as seen in the phase diagram (Fig. 1). In the L64/water solutions, the spectra are of the motionally averaged type at 325 K.

For 5DSA at 325 K in L64/NaOH containing 70% (w/w) polymer (Fig. 2C) the shoulder indicated by the thick upward arrow suggests the presence of an additional component that is similar to that detected for the solution containing 90% (w/w) polymer (L₂ phase); we therefore propose that this sample represents a region where L₂ and L_α phases coexist. The difference with respect to the composition shown in Fig. 1 (only the L_α phase) could be due to slight variations in the polymer samples measured (for instance a different molecular weight distribution), or to the presence of NaOH.

The a_N values at 325 K were calculated directly from the spectra in the L64/water system and from the A_{\max} and A_{\min} values in the L64/NaOH system; the results are presented in Table 1. We note the large difference in a_N values depending on the solvent: 14.4 ± 0.1 G in L64/water and 14.8 ± 0.15 G in L64/NaOH.

An implicit assumption in the interpretation of the ESR spectra for the 5DSA probes is that in L64 solutions the probe is preferentially intercalated in the polymer aggregates

⁵ Ref. [33] has demonstrated that it is possible to control the location of the spin label in a lipid–protein system by variation of the pH. Moreover, the local pK_a was deduced from the relative intensity of spectral components corresponding to the protonated and deprotonated forms of the spin probe.

and not distributed between the water phase and the aggregates; the absence of the sharp lines typical of the probes in neat water (lowest spectra in the four sets presented in Fig. 2) in the spectra of the probes in the polymer solutions is proof that this assumption is correct.

(b) *10DSA*. The broad line assigned to probe aggregation for 5DSA/NaOH is not detected for 10DSA, as seen in the ESR spectra measured at 300 K (Fig. 3A) and at 325 K (Fig. 3C); this result is taken as an indication that the concentration of 10DSA is below the CMC. Since all probe concentrations are essentially the same, this result indicates that $\text{CMC}(10\text{DSA}) > \text{CMC}(5\text{DSA})$; our previous studies in perfluorinated [26,27,32] and protiated [34,35] ionomer systems have detected a similar behavior. The distribution of the probes between the water phase and the aggregates is also affected by the higher CMC of 10DSA probes, compared to 5DSA: the weak signals shown by arrows in Fig. 3A for polymer content of 20 and 50% (w/w) in L64/NaOH and for polymer content of 20% (w/w) in L64/water, represent probes dissolved in water, or associated with isolated chains or with unimeric micelles. Based on a similar spectral contribution in the ionomers [32,34,35], we estimate that the amount of probe in the water, or associated with single chains or unimeric micelles, is negligible: $\leq 1\%$ of the total amount. The signals due to 10DSA in the water phase or near single polymer chains are not detected at 325 K, Fig. 3C and D; the absence of these signals means that the probe distribution at 325 K is dictated by the higher hydrophobicity of the polymer at the higher temperature. Therefore, the ESR spectra represent probes intercalated in the aggregates and not an average of contributions from two or more probe sites.

The presence of NaOH has a less pronounced effect on the ESR spectra of 10DSA, compared to the effect described above for 5DSA; only small differences are seen at 325 K, Fig. 3c, for L64 contents of 20 and 50% (w/w). The a_N values for the 10DSA probes (Table 1) are within experimental error the same in L64/water and L64/NaOH, $a_N \approx 14.3 \pm 0.15$ G.

(c) *10DSE*. This probe is insoluble in neat water and in the NaOH solution, as seen by the very broad lines detected at 300 and 325 K (Fig. 4, bottom spectrum in each set). The presence of NaOH has essentially no effect on the line-shapes measured in the presence of L64 at both temperatures. The only exception is evident in the solution containing 20% (w/w) L64: the higher spectral anisotropy in L64/NaOH, compared to the L64/water systems, is most likely due to a more structured micellar phase. The a_N value for the probe in the L64 solutions at 325 K is the same, 14.3 G, in all solutions, similar to that for 10DSA.

3.2. Local hydration in L64 aggregates

The data presented in Table 1 indicate that for a given probe the a_N values in the same solvent (water or 0.1 M NaOH) at 325 K are independent of L64 concentration:

14.8 G for 5DSA/L64/NaOH, 14.4 G for 5DSA/L64/water and 14.3 G for 10DSA and 10DSE in neat water and in NaOH solutions. Several conclusions can be deduced from these numbers. First, the different a_N values for 5DSA/L64/NaOH and 5DSA/L64/water are representative of sites with different local polarities, higher in L64/NaOH. We can justify this result by assuming that in 5DSA/L64/NaOH the COO^- group of the probe is anchored at the more hydrated (and more polar) regions of the polymer aggregates, compared to the undissociated acid form; additional support for this idea is presented in Fig. 5 (vide infra). Second, as we also expect anchoring of the head group in 10DSA/L64/NaOH in the more hydrated regions of the aggregates (as for 5DSA), the lower a_N value for 10DSA/L64/NaOH (14.3 G) must be due to the different positions of the doxyl groups relative to the head group in 5DSA and in 10DSA. The maximum length of the probes, l_{max} , can be estimated from $l_{\text{max}} = 1.5 + 1.265m$, where m is the number of carbon atoms [36] the distance from the head group to the doxyl group is ≈ 8 and ≈ 14 Å for 5DSA and 10DSA, respectively. The different a_N values for 5DSA and 10DSA suggest that, in the range of depths covered by the nitroxide moiety in the two probes, the hydration changes significantly. Moreover, the local hydration explored by 5DSA/L64/water is similar to that of 10DSA/L64/NaOH. Third, the fact that for 10DSA the a_N values in water and NaOH solutions are about the same indicates an essentially constant hydration level below a depth of ≈ 14 Å from the location of the headgroup. This conclusion is supported by the a_N values for 10DSE, a probe that is not expected to be anchored in a region of higher degree of hydration; this probe selects a location deeper in the hydrophobic regions, but the hydration is the same as for 10DSA [37].^{6,7}

In order to establish a quantitative relation between a_N and the local hydration, we have used the variation of a_N values at 325 K for 5DSA with water content (Fig. 5) in aqueous solutions of the homopolymers PEO and PPO and in a PEO/PPO mixture that mimics the monomer composition of L64. Since these solutions are expected to be homogeneous on the molecular level, the measured a_N values reflect the stoichiometric hydration level expressed as Z . In the L64 solutions, however, the *effective* hydration, Z_{eff} , is a local property determined by the type of aggregation. The calibration curves in Fig. 5 make possible the determination of the real local hydration, Z_{eff} , in the L64 system from the a_N values. For $Z = 0$ (in the neat homopolymers) the a_N values are 14.60 G in PEO, 14.40 G in PPO and 14.45 G in the PEO/PPO mixture; the a_N values

⁶ This chapter gives a simple but lucid description of the polarity effect on the magnetic parameters on nitroxide probes and shows in Fig. 26 (p 501) the increase of both a_N and A_{zz} with increasing solvent polarity.

⁷ Fig. 9 in Ref. [23] shows the proposed polarity profile in reverse micelles of L64 in water/*o*-xylene mixtures, deduced from the a_N values of cationic and *n*DSA spin probes.

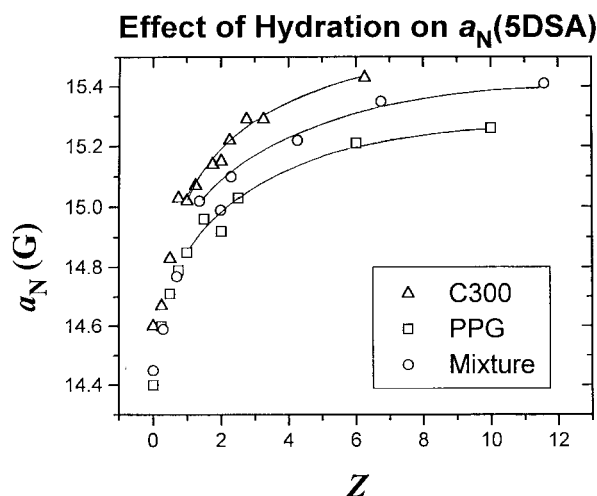


Fig. 5. Variation of a_N for 5DSA as a function of water content, Z , in Carbowax300 (Δ), in PPG425 (\square) and in a mixture of Carbowax300/PPG425 containing the monomer molar ratio 26/30 (\circ). For clarity a_N data points at higher Z values were connected, as a guide to the eye.

of 5DSA in neat water and in the 0.1 M NaOH solution are the same, 15.80 G. Some deductions on the local polarity and hydration will now be made by reading the effective polarity Z_{eff} in the L64 system from the a_N values, by reference to the calibration curves for a_N presented in Fig. 5.⁸

The very low a_N values for the n DSA probes in L64 solutions compared to the values in neat water indicate a very low level of hydration at the probe sites. For $a_N = 14.8$ G, as measured for 5DSA/L64/NaOH, we deduce $Z_{\text{eff}} = 0.5$ –1 in all L64 phases; this value is close to the stoichiometric hydration level, Z , for the L_α and L_2 phases [23], but much lower than that for the L_1 phase, even if the Z value is related to *all* polymer units. For clarity we added in Table 1 the stoichiometric hydration level Z calculated by assuming that the water is associated with EO units only. In the L_1 phase containing 20% (w/w) L64, $Z = 24.8$ when calculated for the EO units only, 21.5 for the PO units only and ≈ 11.5 if all monomers (EO + PO) are considered; these values are much higher compared to the *effective* hydration, Z_{eff} .

The a_N values for all probes in pure L64 are lower than in pure PEO and close to the a_N value in pure PPO (14.40 G). That the probes prefer the environment of PPO is clear from the calibration curve given in Fig. 5, where at low Z values the a_N values are essentially the same in the mixture and in pure PPO. We must conclude that the probes explore and provide evidence for the presence of PO regions of the

⁸ One reviewer recommended that in order to mimic as closely as possible the behavior of L64, the PEO and PPO mixture should be composed of homopolymers with the same length as in the L64 copolymers, in order to minimize the effect of the $-\text{OH}$ end groups on the local polarity. We agree with this point of view. However, the PPO block in L64 has a molecular mass of 1740 and such a PPO polymer is not expected to be soluble in water. The molecular masses we chose are lower than in L64, but are expected to give us the trend in L64 in terms of probe behavior and location.

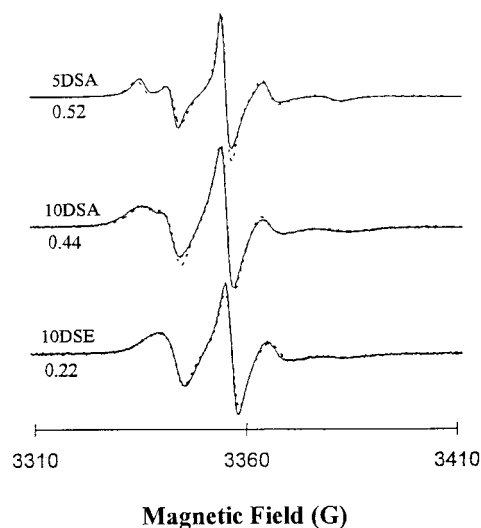


Fig. 6. Experimental ESR spectra at 300 K for the indicated probes (full lines) and simulated lineshapes (dashed lines) with the order parameter, S , given for each probe. The following parameters were used in the simulations: For 5DSA $R_\perp = 2 \times 10^7$ rad/s, $R_\parallel = 1 \times 10^{10}$ rad/s, $\psi = 27^\circ$; for 10DSA $R_\perp = 4 \times 10^7$ rad/s, $R_\parallel = 1 \times 10^8$ rad/s, $\psi = 30^\circ$; and for 10DSE $R_\perp = 4 \times 10^7$ rad/s, $R_\parallel = 1 \times 10^8$ rad/s, $\psi = 30^\circ$. All spectra were calculated with a linewidth of 0.50 G.

aggregates and the effect of NaOH is to force the headgroup of the 5DSA and 10DSA probes into the more hydrated EO regions. The $>\text{NO}$ group in 5DSA/L64/NaOH is at a distance of ≈ 8 Å from the hydrated EO regions but inside the non-hydrated PO regions of the polymer aggregates. This major conclusion is in accord with previous studies of the binary and ternary reverse micellar phase in L64 with n DSA probes [23] and of all phases in aqueous L64 with cationic spin probes [24].

Further details about the nature of the sites reported by the spin probes were obtained by measuring ESR spectra of 5DSA/L64/NaOH at 325 K in the 70% (w/w) L64 solution (lamellar phase) as a function of the amount of added cholesterol (up to 10% mol, the maximum amount that can be dissolved); the spectra are essentially the same and the corresponding a_N values are in the range 14.8–14.9 G; the results at 300 K are similar. Cholesterol is expected to lead to the intercalation of the n DSA spin probes deeper inside the hydrophobic regions [38]. The probe site is not affected by cholesterol addition, because its headgroup is anchored at a hydrated site and not in the most hydrophobic part of the aggregates, in accord with deductions made from the calibration curve in Fig. 5.

3.3. The order parameter in the lamellar phase

To determine the order parameter, we simulated the ESR spectra of the three probes at 300 K using the microscopic order–macroscopic disorder (MOMD) model, which assumes that in a given domain the director is uniformly oriented in space (“microscopic order”) while the morphology consists

of a random distribution of the oriented domains (“macroscopic disorder”). The parameters needed for simulating the lineshapes are: the components of the rotational diffusion tensor, R_{\parallel} and R_{\perp} ; the order parameter, S ; the diffusion tilt angle, ψ ; and the linewidths. The motional model chosen was the Brownian diffusion model [28–30].

In Fig. 6 we present simulated (dashed lines) and experimental (solid lines) spectra for the indicated spin probes at 300 K in the L64/NaOH system and the corresponding order parameter S . The parameters used for the simulations are shown in the caption. S decreases from 0.52 for 5DSA, to 0.44 for 10DSA and to 0.22 for 10DSE; these numbers suggest that a gradient of order exists in the aggregates, with more disorder in the hydrophobic interior.⁹ The parameters used for the simulations provide additional support for both the location of the probes and the local hydration proposed above: While the ψ values for the three probes are similar (27, 30 and 30°, respectively, for 5DSA, 10DSA and 10DSE, see caption of Fig. 6), there are important differences in the R_{\perp} and R_{\parallel} values. The largest difference is in the R_{\parallel} values: 1×10^{10} rad/s for 5DSA and 1×10^8 rad/s for both 10DSA and 10DSE. The significantly higher R_{\parallel} value for 5DSA is in agreement with the higher hydration at the site of this probe, as deduced from both the lineshapes and the a_N values. The (smaller) difference in the R_{\perp} values for 5DSA compared to 10DSA and 10DSE can be a reflection of the higher order parameter at the 5DSA location.

4. Conclusions

The ESR spectra of the probes reflect hydrophobic sites where the hydration is very low (5DSA) and where the hydration is essentially zero (10DSA and 10DSE), respectively. The calibration curves of a_N indicated that these sites consist of non-hydrated PO blocks [37]. Simulations of the ESR spectra in the lamellar phase reflect an order parameter that decreases gradually from the EO/PO interface into the PO domains. Since the non-polar PO region is ≈ 40 Å thick, the amphiphilic probes studied report on an intermediate domain which is ≤ 8 Å thick and PO domain of thickness ≥ 30 Å. These deductions are in accord with the hydration gradient deduced in L64 aggregates from the ESR spectra of cationic probes.

While the study based on cationic probes reported on the hydration gradient in the EO domains and the very low hydration near the EO/PO interface [24], the present results provide evidence for the existence of PO domains with zero effective local hydration.

⁹ In the preliminary report, Ref. [25], we placed the COO^- group of the 5DSA and 10DSA spin probes at the interface between water and EO blocks, because at that time we did not measure the a_N values of 5DSA in PPO or the PEO/PPO mixture. From the additional data in the present study we deduced that the COO^- group is anchored at the interface between the PO and EO blocks.

Acknowledgements

This research was supported by the Polymers Program of the National Science Foundation. The authors thank A. Caragheorghopol (Bucharest) and J. Pilar (Prague) for numerous discussions; J. Otten of BASF for the gift of the Pluronics; G. C. Rex of Union Carbide for the Carbowax samples; and ARCO Company for the PPG425 samples. We appreciate the contribution of the three referees who by their useful comments and constructive criticism helped us in improving the content and clarity of the paper.

References

- [1] Alexandridis P, Hatton TA. *Colloids Surf A* 1996;96:1.
- [2] Almgren M, Brown W, Hvidt S. *Colloid Polym Sci* 1995;273:2.
- [3] Schmolka IR. In: Schick MJ, editor. *Non-ionic surfactants*. New York: Marcel Dekker, 1967 chap 10.
- [4] Schmolka IR. *J Am Oil Chem Soc* 1977;54:110.
- [5] Pluronic and Tetronic Surfactants. Technical Brochure. BASF Corp., Parsippany, NJ, 1989.
- [6] Chu B, Zhou Z. *Non-ionic surfactants*. New York: Marcel Dekker, 1996. p. 67 chap 3.
- [7] Alexandridis P, Lindman B, editors. *Amphiphilic block copolymers: self-assembly and applications*. Amsterdam: Elsevier, 1997.
- [8] Alexandridis P, Olsson U, Lindman B. *J Phys Chem* 1996;100:280.
- [9] Zhang K, Khan A. *Macromolecules* 1995;28:3807.
- [10] Alexandridis P, Olsson U, Lindman B. *Macromolecules* 1995;28:7700.
- [11] Alexandridis P, Zhou D, Khan A. *Langmuir* 1996;12:2690.
- [12] Wu W, Zhou ZK, Chu B. *Macromolecules* 1993;26:2117.
- [13] Wu W, Chu B. *Macromolecules* 1994;27:1766.
- [14] Zhou S, Chu B. *J Polym Sci Part B* 1998;36:889.
- [15] Andersson M, Karlstrom G. *J Chem Phys* 1985;89:4957.
- [16] Linse P. *Macromolecules* 1993;26:4437.
- [17] Hurter PN, Scheutjens JM, Hatton TA. *Macromolecules* 1993;26:5030.
- [18] Alexandridis P, Holtzwarth JF, Hatton TA. *Macromolecules* 1994;27:2414.
- [19] Medhage B, Almgren M, Alsins J. *J Phys Chem* 1993;97:7753.
- [20] Baglioni P, Bongiovanni R, Rivara-Minten E, Kevan L. *J Phys Chem* 1989;93:5574.
- [21] Caragheorghopol A, Caldararu H, Dragutan I, Joela H, Brown W. *Langmuir* 1997;13:6912.
- [22] Malka K, Schlick S. *Macromolecules* 1997;30:456.
- [23] Caragheorghopol A, Pilar J, Schlick S. *Macromolecules* 1997;30:2923.
- [24] Caragheorghopol A, Schlick S. *Macromolecules* 1998;31:7736.
- [25] Zhou L, Schlick S. *Polym Prepr (Am Chem Soc Div Polym Chem)* 1996;37:829.
- [26] Szajdzinska-Pietek E, Schlick S, Plonka A. *Langmuir* 1994;10 1101 and 2188.
- [27] Szajdzinska-Pietek E, Pilar J, Schlick S. *J Phys Chem* 1995;99:313.
- [28] Meirovitch E, Nayeem A, Freed JH. *J Phys Chem* 1984;88:3454.
- [29] Meirovitch E, Freed JH. *J Phys Chem* 1984;88:4995.
- [30] Schneider DJ, Freed JH. In: Berliner LJ, Reuben J, editors. *Biological magnetic resonance. Spin labeling*, 8. New York: Plenum Press, 1989 chap 1.
- [31] Haering G, Luisi PL, Hauser H. *J Phys Chem* 1988;92:3574.
- [32] Szajdzinska-Pietek E, Schlick S. In: Schlick S, editor. *Ionomers: characterization, theory and applications*. Boca Raton, FL: CRC Press, 1996 chap 7.
- [33] Horvath LI, Brophy PJ, Marsh D. *Biochemistry* 1988;27:5296.

- [34] Kutsumizu S, Hara H, Schlick S. *Macromolecules* 1997;30:232.
- [35] Kutsumizu S, Schlick S. *Macromolecules* 1997;30:2329.
- [36] Romanelli M, Ristori S, Martini G, Kang Y-S, Kevan L. *J Phys Chem* 1994;98:2125.
- [37] Griffith OH, Jost PC. In: Berliner LJ, editor. *Spin labeling I. Theory and applications*. New York: Academic Press, 1976 chap 12.
- [38] Bratt PJ, Kevan L. *J Phys Chem* 1993;97:7371.